Considerations in the Use of the Laser Flash Method for Thermal Measurements of Thermal Interface Materials

Vinh Khuu, *Member, IEEE*, Michael Osterman, *Member, IEEE*, Avram Bar-Cohen, *Fellow, IEEE*, and Michael Pecht, *Fellow, IEEE*

***Abstract*— With increasing thermal fluxes, the performance of thermal interface materials (TIMs) that are used to reduce the thermal resistance between contacting surfaces in electronic devices, such as at the die-to-heat sink or heat spreader-to-heat sink interfaces, is becoming critical. However, measuring the thermal resistances of TIMs in a manner representative of actual applications is difficult. The laser flash method is a technique that may be used to determine the thermal resistance of TIMs and their degradation under environmental exposure. This paper examines three issues associated with using the laser flash method that could limit its effectiveness in calculating thermal resistance: sample holder heating, clamping, and error in the Lee algorithm outputs due to coupon–TIM thermal diffusivity differences. As a case study, the thermal performance of polymer TIMs in pad form, as well as an adhesive and a gel, were examined. Finite element simulations indicated that, without proper consideration, sample holder heating can lead to significant error in the calculated TIM thermal conductivity values.**

***Index Terms*— Degradation, laser flash method, reliability, thermal interface materials.**

NOMENCLATURE

R	Thermal resistance.
k	Thermal conductivity.
BLT	Bond line thickness.
α_{CTE}	CTE.
τ	Shear stress decay time.
G	Shear modulus.
T	Temperature.
l	Length.
E	Young's Modulus.
A	Cross-sectional area.
ν	Poisson's ratio.
$t_{1/2}$	Half-rise time.
L	Thickness.
α	Thermal diffusivity.
η_i	Square root of the heat diffusion time.
H	Volumetric specific heat.
V	Normalized temperature.

Manuscript received November 9, 2009; revised July 8, 2010; accepted November 15, 2010. Date of current version July 20, 2011. Recommended for publication by Associate Editor R. Prasher upon evaluation of reviewers' comments.

V. Khuu is with Schlumberger, Sugar Land, TX 77478 USA (e-mail: vkhuu@umd.edu).

M. Osterman, A. Bar-Cohen, and M. Pecht are with the Center for Advanced Life Cycle Engineering, University of Maryland, College Park, MD 20742 USA (e-mail: osterman@calce.umd.edu; abc@umd.edu; pecht@calce.umd.edu).

Color versions of one or more of the figures in this paper are available online at http://ieeexplore.ieee.org.

Digital Object Identifier 10.1109/TCPMT.2011.2112767

I. INTRODUCTION

DUE TO increasing power dissipation levels occurring in a variety of microelectronic applications, the thermal resistance between the die and the ambient environment can play a significant role in maintaining component operating temperatures at acceptable levels. Only 1–2% of the apparent areas of two joined solid surfaces are in physical contact due to the imperfect contact interface caused by gaps and asperities [1]. Thermal interface materials (TIMs) may be inserted between two solid interfacing surfaces to reduce the thermal impedance between a heat-generating component and a heat sink. In electronic systems, resistance through the TIM layer can account for 30–50% of the total thermal resistance budget [2]. In many applications, such as military, space, and automotive, TIMs can be exposed to high temperature, humidity, or vibration for the extended periods. Degradation in the performance of the TIM during its operating life can affect system thermal performance [3]–[6] and potentially lead to premature failure of the device in some instances.

While considerable progress has been made in understanding factors governing thermal contact resistance and the performance of TIMs [1], [7], [8], fundamental physics-based models have yet to be developed to describe TIM degradation [1]. Data on TIM reliability are often not provided by vendors [9], but measurement techniques for characterizing bulk material thermal performance often yield data that are inconsistent [2], [10]. With perhaps the exception of studies examining the degradation of thermal greases [4], [11]–[13], the long-term behavior of many types of TIMs, such as polymer TIMs in pad form, remains relatively unexplored in the literature. Improved methods for accurately capturing the response of a TIM to environmental stress conditions are therefore required to better understand conditions that lead to degradation.

Methods for testing TIMs include use of test vehicles, which contain heating elements, temperature sensors, and dummy processors designed to simulate TIM usage conditions [14]–[17]. Another method involves material conductivity test systems, such as those based on the ASTM D5470 test standard [10], [18]–[20], which are commonly used by TIM vendors but usually do not allow environmental conditions,

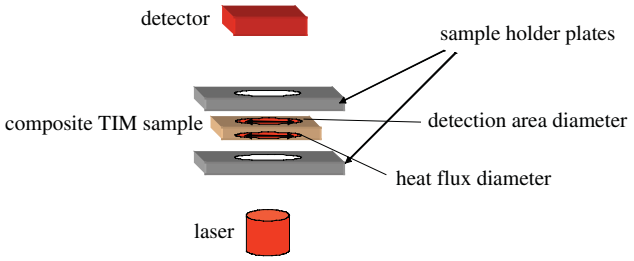

Fig. 1. Illustration of the laser flash method.

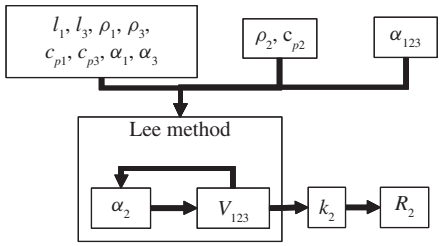

Fig. 2. TIM thermal resistance measurement and calculation.

such as temperature, humidity, and vibration, to be easily controlled.

The laser flash method, which is an established technique for determining the bulk material properties of thin solid test specimens, including the thermal conductivity, has an advantage over steady-state techniques because of the noncontact nature of the measurement. The laser flash method has been used to study solders, adhesives, and thermal greases [11], [21], [22]. However, one common criticism of this technique is that test specimens, which must be exposed to the ambient environment on the top and bottom during a measurement, do not simulate loading conditions in typical TIM applications. Some have also noted that, since other thermal and mechanical properties need to be known in order to determine the conductivity, the "stack up" of uncertainties caused by the laser flash method can lead to large errors. The laser flash method is also difficult or impossible to use when coupons/substrates and the TIM samples have large differences in thermal diffusivity [16]. These criticisms have not yet been thoroughly examined in the literature, and many questions remain as to how to apply the laser flash method to obtain accurate and useful thermal resistance data that can yield information about the reliability of TIMs.

The laser flash method has come into widespread use for measuring the bulk thermal conductivity of thin solid homogeneous test samples due to its advantages in terms of measurement speed and sample size. Parker *et al.* [23] proposed the flash diffusivity technique as a means of measuring the thermal diffusivity of a material. Various researchers proposed refinements to describe the heat transfer occurring through the test specimen during the laser flash measurement, including Cowan [24], who modified the Parker model to account for heat loss in the test sample due to radiation, and Clark and Taylor [25], who used similar assumptions as Cowan but focused on the heating part of the temperature rise curve to determine thermal diffusivity. These methods differ from the Parker method in how the thermal diffusivity is calculated from a measured temperature rise curve.

The laser flash method involves monitoring the temperature of the rear surface of a test sample after a burst of energy (supplied by a laser) heats the front surface of the sample and the resulting temperature rise propagates through the material. The temperature rise curve, usually measured by an infrared (IR) detector, yields the thermal diffusivity of the test sample as well as the specific heat when a reference measurement is also performed. The basic configuration is illustrated in Fig. 1. When the thermal diffusivity and specific heat are known, the thermal conductivity can be calculated using the definition of the thermal diffusivity ($\alpha = k/\rho \times cp$). In this paper, the thermal diffusivity was determined using the Koski procedure, which requires time and temperature ratios of various points along the temperature rise curve [26]. The Koski procedure was used in conjunction with Cowan's method, which focuses on temperatures following the peak of the temperature rise profile.

The laser flash method can provide an indirect thermal resistance measurement across a multilayer TIM test sample. The TIM thermal resistance is derived from the thermal diffusivity measurement. For this paper, an algorithm developed by Lee [27] and Lee [28] was used to calculate the thermal resistance across the TIM layer based on the properties of the individual layers and the three-layer sample. Since interfacial contact resistance cannot be extracted from the three-layer case considered by Lee [28], the thermal resistance calculated from the algorithm includes both bulk and interfacial contact contributions. That is, thermal resistance values reported in this paper are the sum of the contact resistances $R_{contact\,1}$ and $R_{contact\,2}$ at each interface and the bulk resistance of the TIM, as follows:

$$R_{total} = \frac{BLT}{k_{TIM}} + R_{contact\,1} + R_{contact\,2} \tag{1}$$

where BLT is the bondline thickness and k_{TIM} is the bulk thermal conductivity of the TIM layer. Lee's formulation for layered composites relies on several assumptions, including 1-D heat flow, no heat loss from the sample surfaces, homogeneous layers, and constant thermal properties over the temperature range, many of which were examined by Lee [27] and Lee [28]. The half-rise time (the time to reach half of the maximum value) of the temperature response of the composite sample was determined from the apparent diffusivity obtained from the measured data using the relation

$$\alpha = \frac{1.38\,L^2}{\pi^2 \cdot t_{1/2}} \tag{2}$$

where $t_{1/2}$ is the half-rise time, L the thickness, and α the thermal diffusivity. The half-rise times as well as the single-layer properties were then used as inputs for the Lee algorithm. The thermal diffusivity of the TIM layer was iterated until the normalized temperature V using the three-layer composite solution at the half-rise time converged to 0.5. The thermal conductivity was then determined for the converged diffusivity value from the definition of thermal diffusivity. Fig. 2 summarizes the process used to calculate the TIM thermal resistance.

Fig. 3. Illustration of clamped TIM assembly.

In this paper, the laser flash method will be evaluated as a technique for evaluating the thermal conductivity and change in conductivity of selected TIMs. The experimental procedure followed and data obtained will be presented, and the experimental values will be compared with vendor-provided data. Discrepancies between laser flash evaluations and vendor data will be examined through additional experiments and thermal simulations. Structural simulations will be used to examine how clamping affects the TIM bondline thickness as well as the ability of laser flash test structures to simulate realistic loading conditions. Errors in the Lee algorithm outputs due to coupon/TIM thermal diffusivity differences will be examined numerically.

II. Laser Flash Experimental Approach

To experimentally measure the thermal resistance of the selected TIMs, the TIMs were sandwiched between two metal coupons held by a specimen holder, which consisted of two holder plates connected by four screws, as depicted in Fig. 3.

A typical test sample clamped with holder plates is depicted in Fig. 4. Aluminum and Lexan were used to construct holder plates.

In this paper, 1-mm-thick copper and alloy 42 coupons were used. The coupon materials, i.e., oxygen-free high conductivity copper and alloy 42, were selected on the basis of the differences in their coefficients of thermal expansion (CTEs) in order to increase the maximum shear stress applied to the TIM. All sample coupons of a given material were fabricated from the same lot to prevent variations in surface roughness between samples from affecting the measurements. The copper coupons are shown with dimensions in Fig. 5. The alloy 42 coupons had the same dimensions.

The sample holder plates in this paper allowed the three-layer test specimens to remain undisturbed between laser flash measurements and periods of environmental exposure. Ideally, the plates should not have affected the flow of heat through the three-layer test specimen during the laser flash measurement. Laser flash data from multiple test samples were compared with that of vendor datasheet values to examine the impact of clamping on the TIM specimen and coupon size on the laser flash measurement. Additional experiments examined the impact of varying the coupon size and shape and the sample holder plate material to evaluate the effect of heating of the sample holder plates on the measured TIM thermal conductivity values. The approach outlined in this section describes the procedure for determining the effective TIM thermal conductivity and thermal resistance based on laser flash measurements for all laser flash tests.

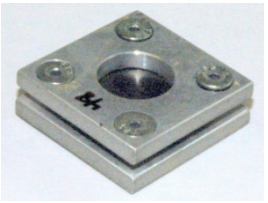

Fig. 4. Typical assembled test sample holder.

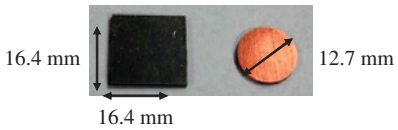

Fig. 5. Test specimen coupons (copper).

A. Laser Flash Test Procedure Overview

For the laser flash measurements, the density of the TIM layer was calculated by measuring the mass of the sample and the coupons and assuming that the TIM covered the entire face of the coupon (neglecting the material squeezed out when compressed). The Lee algorithm [27], [28] also requires specific heat values of the individual layers of the composite sample. Thus, the vendor value of the TIM layer specific heat was used in the thermal resistance calculation for all samples except the adhesive and gel samples, which required differential scanning calorimetry (DSC) measurements to be performed. Due to the difficulty in applying the graphite coating to single-layer polymer TIMs, DSC was used for determining the specific heat in samples where vendor data were not provided. DSC is a thermoanalytical technique in which the difference in the amount of heat required to increase the temperature of a sample and reference is measured as a function of temperature. It is generally a more accurate technique for measuring specific heat than the laser flash method, as there is no variability in heat pulses between successive runs or no dependence on coating material or sample surface properties [29]. Values of the thermal diffusivity of the coupon layers, which are also needed in the Lee algorithm, were determined from reference handbooks or the specific heat and thermal conductivity values provided by the vendor. Measured values for specific heat and thermal diffusivity were used for the coupon layers and assumed to be the same among all the samples.

All laser flash measurements were performed at room temperature. Although it can be shown that the value of the TIM layer thermal resistance is not dependent on which side faces the laser [28], all laser flash measurements were conducted with the copper side facing the laser beam in order to avoid variation due to the coupon surface finishes. The area of the sample irradiated by the laser was 5.9 mm in diameter. The temporal pulse width was approximately 0.3 ms in duration. The sample temperature rise was not determined during laser flash measurements, which used temperature normalized by the maximum temperature, but was likely in the order of a few degrees kelvin in magnitude based on laser flash literature. Five flashes were imposed per measurement, as was

recommended by the instrument manufacturer. A 50% optical filter, which has the highest transmittance available for this instrument, was used in the measurements to attenuate the beam power. In preliminary trials, the Cowan [24], Clark and Taylor [25], and Parker [23] methods were compared. In most cases, little difference was found between results generated by the Cowan and Clark and Taylor methods. However, in some instances, the Clark and Taylor method could not be used perhaps because of the low signal-to-noise ratio. In preliminary measurements in this paper, the Parker method often yielded poor fits with the experimental data, perhaps because of the assumption of no heat loss during the cool-down phase. Because of these considerations and for consistency, the Cowan method was used to determine the thermal diffusivity of all the samples. It is to be noted that, when all three techniques were compared, the Cowan method generally led to lower values of thermal conductivity as compared to values derived from the Parker and the Clark and Taylor methods.

B. Laser Flash TIM Samples and Sample Holder

The test samples examined in this paper included thermal gap pads and gap fillers, putties, an adhesive, and a gel. Test samples were chosen to represent a range of TIMs, and specific samples within a product line were selected on the basis of the thickness constraints of the sample holder. Silicone and non-silicone gap pads with boron nitride filler were evaluated in this paper along with a silicone gap filler with boron nitride filler. The gap pads had a thin layer of pressure-sensitive adhesive applied to promote adhesion at the interfaces. The thermal gel is a reworkable, diamond-filled, electrically insulating, and thermally conductive silicone paste. Gap putties are similar to gap fillers but have a compression level of greater than 50% of the original thickness. Although all Gap Putty A samples had the same bulk material, some also had a layer of metal foil that was used to allow the putty to be removed after use, as needed in specialized applications. All materials were suitable for so-called TIM 2 (heat spreader or thermal lid to heat sink) applications, although the epoxy adhesive could also be used as a die attachment material (die to substrate). With the exception of the adhesive and gel, all samples were manufactured in pad form. The adhesive and gel were manually dispensed from syringes onto the coupons in an "X" pattern. About 30% compression was applied to the samples in pad form. The test coupons were 16.4 mm in length per side (square) and were composed of Cu and alloy 42. Kapton tape with 0.07 mm thickness was used as a spacer for the gel and adhesive specimens. Table I summarizes the test samples measured.

To simulate realistic loading conditions, laser flash measurements were performed on various TIMs assembled into tri-layer sandwich structures, enabling the test samples to remain undisturbed between measurements performed periodically throughout reliability testing.

C. Laser Flash Test Sample Preparation

The surfaces of the coupons were cleaned with isopropyl alcohol prior to assembling the sandwich structures. Graphite coating was applied to all test sample sandwiches to enhance the absorptivity and emissivity prior to each sequence of laser flash runs. Five coats of graphite were applied in accordance with ASTM E1461 [30] and the laser flash manufacturer's directions. The thermal performance of gap pads and gap fillers, which generally require higher clamping forces for optimal performance, is highly dependent on the force loading [1].

TABLE I
TYPICAL ASSEMBLED TEST SAMPLE HOLDER

Designation	Construction and composition	Vendor thermal conductivity (W/m-K)
Putty A	Alumina-filled silicone	11
Putty B	Boron nitride-filled silicone	3
Putty C	Alumina-filled silicone	6
Adhesive	Diamond-filled non-silicone paste	11.4
Gel	Diamond-filled non-silicone paste	10
Gap filler	Alumina-filled silicone	2.8
Gap pad A	Alumina-filled non-silicone	0.9
Gap pad B	Alumina-filled silicone	2.4

Many manufacturers control contact force when characterizing the thermal performance of their TIMs as per ASTM D5470. But the stresses in viscoelastic TIMs change over time due to their viscoelastic nature. Since bondline thickness can be more accurately controlled than the force, a nominal 25% compression was applied to the gap filler, putty, and gap pad samples during assembly. This thickness value was within the manufacturer's recommended compressed thickness values. The thickness was controlled manually by tightening the sample holder screws and measuring the thickness using a micrometer. Care was taken to ensure that tightening the screws to compress the TIM would result in a uniform thickness and not cause gaps that could result in voids during assembly.

For the epoxy adhesive samples, which were not held under pressure, a 180-μm-thick bondline was maintained using Kapton tape at the corners of the sample. Kapton tape was chosen because of its good stability at high temperature. The amount of adhesive dispensed onto the coupon surfaces was controlled manually by the dispenser before the coupons were mated together. The adhesive samples were cured as per manufacturer's instructions using a 60 °C prebake for 1 h and a 150 °C bake for 0.5 h. For the adhesive samples, the top and bottom aluminum plates of the sample holder were used to mask the laser beam and radiation from the rear sample, and no clamping force was applied by tightening the screws. Sample thicknesses of the gap pads and fillers were measured with a flat point micrometer, which had an accuracy of 0.025 mm, and values were averaged over three thickness measurements of the three-layer test specimen.

TABLE II
COMPARISON OF LASER FLASH MEASUREMENTS WITH VENDOR VALUES

a) Square test coupons

		Putty A (no foil)	Adhesive	Gap filler	Gap pad A	Gap pad B
Thermal Resistance (mm^2K/W)	Vendor	101	22	271	633	213
	Measured	80 ± 5	69 ± 7	125 ± 11	253 ± 42	69 ± 7
	Thickness (mm)	1.1 ± 0.03	0.3 ± 0.02	0.8 ± 0.04	0.6 ± 0.04	0.5 ± 0.02

b) Round test coupons

		Putty A (no foil)	Putty A (with foil)	Putty B	Gap pad A	Gel
Thermal Resistance (mm^2K/W)	Vendor	125	127	467	656	11
	Measured	163 ± 10	229 ± 48	479 ± 31	431 ± 76	41 ± 10
	Thickness (mm)	1.4 ± 0.03	1.4 ± 0.01	1.4 ± 0.01	0.6 ± 0.01	0.5± 0.02

III. MODELING APPROACH

To study potential issues arising from use of the laser flash method on clamped TIM specimens and to explain test measurements in the study reported in this paper and a previous study [31], finite element (FE) models were constructed and simulations were performed. More specifically, the FE model simulations of the laser flash test measurement assessed the impact of the sample holder on the calculated TIM thermal conductivity, while structural simulations examined mechanical loading on TIM test specimens.

A. Thermal Modeling Procedure

In a previous study [31], laser flash measurements of three-layer test specimens clamped between two sample holder plates yielded TIM thermal conductivity values much higher than those reported in vendor datasheets. It was surmised that heating of the sample holder plates was responsible for this discrepancy, but this effect was not investigated in depth in the previous study [31] and is therefore explored here.

The approach used in the finite element analysis (FEA) simulation of the laser flash measurement involved first assuming a value for thermal conductivity of the TIM layer and then applying a transient heat flux to the test specimen to approximate the pulse from the laser that irradiates the test specimen. The half-rise times obtained from the temperature rise curve of the simulated three-layer test sample resulted in thermal diffusivity values, from which TIM thermal conductivity could be determined using the Lee method. Since this value may differ from the initial value of thermal conductivity assumed in the model, the value must be iterated. The FE-based procedure provides a means to quantify error and is not normally used in laser flash measurements. In experiment, the actual TIM k value is unknown, and the Lee method applied to the experimental data yields only a single TIM thermal conductivity value per sample. The FE model was generated assuming no heat conduction to the sample holder plate screws, no radiative heat losses from the test specimen, and isotropic homogeneous material properties. This procedure is summarized in Fig. 6.

For the study reported here, the heat flux was imposed on an area corresponding to the area of the sample holder opening (laser side), and the heat flux was assumed to be uniform over the area of coverage. The area visible to the detector corresponded to the area of the sample holder opening (detector side).

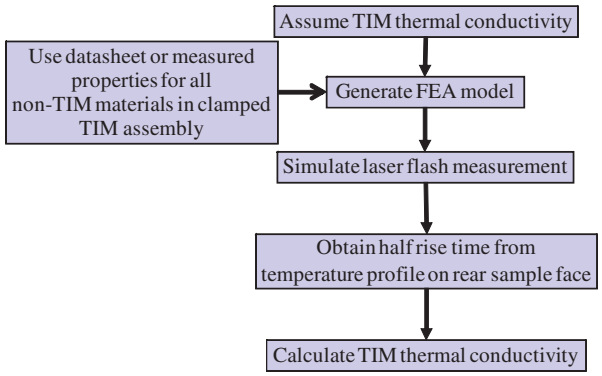

Fig. 6. Overview of TIM thermal conductivity calculation procedure.

B. Structural Modeling Procedure

TIMs experience compression in typical applications due to screws or clips that help ensure good thermal contact between the heat spreader and the heat sink. The laser flash method requires one surface to be exposed to the laser and the other surface to be in view of an IR detector. For the three-layer test specimens, openings on the top and bottom of the sample holder plates, which are required for laser flash measurements, prevented force from being applied uniformly over the top and bottom surfaces of the three-layer TIM sandwich. The purpose of the structural FE analysis in this paper was to assess the effect of any deformation experienced by the TIM layer as a result of the opening in the sample holder plates that clamp the TIM. The results would help determine how well the TIM laser flash test fixtures approximate typical TIM application loading conditions, which are assumed to result in a uniform bondline thickness.

TIMs in this paper were assumed to exhibit linear viscoelastic behavior. The generalized Maxwell model approximates linear viscoelastic behavior as a series of springs and dashpots in parallel [32]. Mechanical material

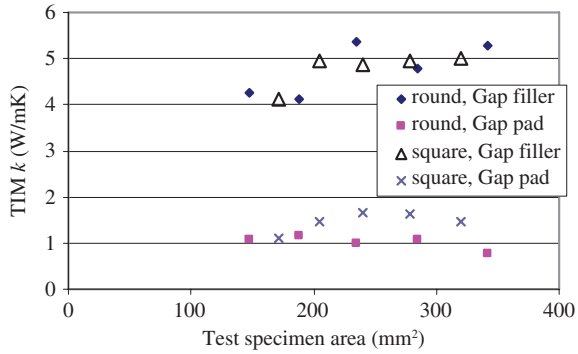

Fig. 7. Effect of area on TIM thermal conductivity based on the laser flash measurements.

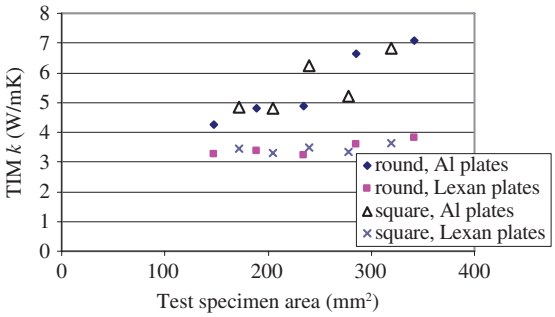

Fig. 8. Effect of area on TIM thermal conductivity based on the laser flash measurements of gap filler.

properties can be represented using the kernel function of generalized Maxwell elements expressed in terms of the Prony series as follows [32], [33]:

$$G = G_\infty + \sum_{i=1}^{n_G} G_i \exp\left(-\frac{t}{\tau}\right) \tag{3}$$

where G is the elastic shear modulus and τ is the relaxation time for each Prony component. The viscoelastic material properties were determined using Prony series fits with five terms. Assuming the material was isotropic, the shear modulus (G) was determined from elongation modulus (E) data [33], using $\nu = 0.49$ [33], the isotropic material assumption, and the following relation:

$$G = \frac{E}{2(1+\nu)} = \frac{E}{2.98}. \tag{4}$$

To measure the material properties of the TIM layer used in the FE models, stress relaxation tests were conducted using dynamic mechanical analysis (DMA). Input properties for the sample holder plates and coupons were based on reference handbook values. Simulations were performed with and without the openings in the sample holder plates used for laser flash measurements, keeping all other parameters constant to examine the impact of the opening on TIM deformation.

IV. Laser Flash Experimental Results

Laser flash measurements on multiple TIM samples were carried out using square and round test coupons, as summarized in Table II. Vendor values of thermal resistance were based on TIM thermal conductivity datasheet values using as-assembled thickness values of the test specimens. Laser flash data generally yielded moderately lower thermal resistances than those based on vendor datasheet values, but for clamped square specimens, which used samples much larger than the opening, the differences were up to a factor of three. Differences with vendor values and discrepancies among laser flash measurements performed on the same TIM suggested that test coupons in combination with the sample holders might be contributing to error.

The largest differences with vendor values can be attributed to sample holder plate heating, but even with the round specimens there may still have been some amount of plate heating. Square samples in pad form generally showed the lowest resistances compared to their corresponding vendor values. Plate heating may have played a greater role for the gap pads due to the higher contact pressures resulting from the reinforcement in the gap pads, which are not present in the fillers and putties. Lower contact pressures in the tests compared to that of vendor test conditions would explain the higher resistances, as seen in the Putty A results for the round coupons. Difference in the high-temperature cure and cross-linking during sample preparation can contribute to differences with vendor data, which can explain the higher resistances seen in the gel and adhesive.

To evaluate the impact of radial heating and sample holder plate heating effects, five round samples of varying radii and five square samples of varying side length of gap pad A and gap filler were measured at a compression level between 5 and 10% using aluminum for the sample holder plates. The experimental uncertainty was determined to be approximately 15–20% based on the analysis from Section VI. In examining area as a parameter, these measurements showed that a square TIM specimen larger than the opening could increase the calculated TIM thermal conductivity, while the round specimens did not show this trend, and in some cases a higher radius led to a lower calculated TIM layer thermal conductivity. Gap pad A TIMs did not show a clear increase in measured TIM thermal conductivity with increasing sample area as would be expected from radial heating assumptions and previous measurements. These results are summarized in Fig. 7. It was also seen that, with increasing sample area, the signal also decreased. And for samples with larger radii or side lengths, the temperature profiles had lower signal-to-noise ratios, indicating that these data points may not be suitable for establishing a trend.

For measurements of the same TIM (gap filler) varying the plate material, as shown in Fig. 8, use of aluminum holder plates resulted in higher measured TIM thermal conductivity values than those obtained using Lexan plates. The increase in measured TIM thermal conductivity with increasing area (slope) was higher in tests conducted using aluminum holder plates than those conducted using Lexan plates. These trends indicate that sample holder material plays a dominant role in increasing the measured TIM thermal conductivity and that radial conduction effects may be small in comparison.

Additional tests to examine the impact of each plate individually, in which both Lexan and aluminum were used for

TABLE III
TIM THERMAL CONDUCTIVITY BASED ON LASER FLASH MEASUREMENTS WITH ALUMINUM AND LEXAN SAMPLE HOLDER PLATES

Test specimen area (mm^2)	Bottom plate (toward laser)	Top plate (toward detector)	Measured TIM thermal conductivity (W/m-K)
342 (round)	Al	Al	7.1
342 (round)	Lexan	Al	4.9
342 (round)	Al	Lexan	4.7
342 (round)	Lexan	Lexan	3.8
320 (square)	Al	Al	6.8
320 (square)	Lexan	Al	5.2
320 (square)	Al	Lexan	5.1
320 (square)	Lexan	Lexan	3.6

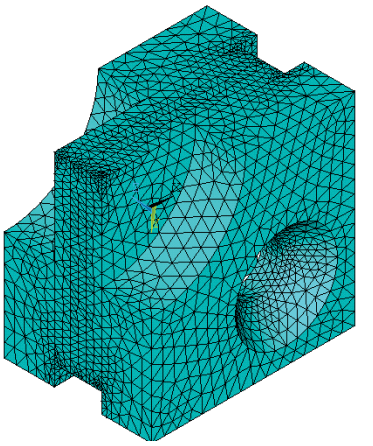

Fig. 9. Thermal FE mesh.

sample holder plates during the same measurements yielded data to distinguish between the relative contributions of each plate to the increase of the measured TIM thermal conductivity, as summarized in Table III. Heat flow into the top and bottom sample holder plates appears to have contributed equally to the increase in apparent measured TIM thermal conductivity, suggesting that heating of both sample holder plates led to increased measured TIM thermal conductivity values.

V. LASER FLASH MODELING RESULTS

The thermal FE models generated in this section were used to simulate the three-layer test specimen and the sample holder plates used to clamp the three-layer test specimen. The screws holding the sample holder plates together were neglected.

A. Thermal FE Simulations

To examine why experimental laser flash results depended on the sample holder plate material and explain how sample holder plate heating affected laser flash data used to determine TIM thermal conductivity values, transient thermal FE models of the assembled TIM structures were generated using aluminum or Lexan as the sample holder plate materials. Simulations were also performed for a configuration with no sample

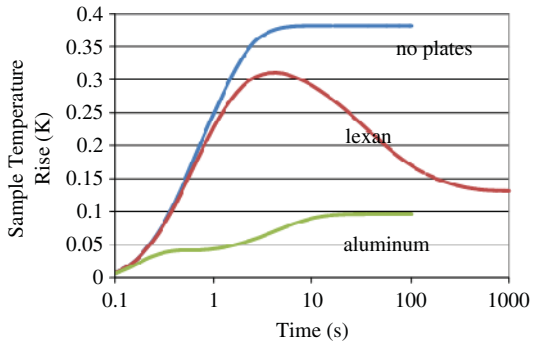

Fig. 10. Temperature rise profiles from laser flash simulations.

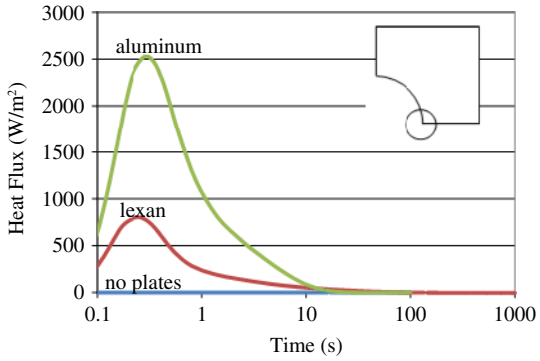

Fig. 11. Local heat flux profile on top clamping plate (coupon side) from laser flash simulations.

holder plates. The pulse from the laser was approximated as a 15-J transient heat flux with a triangular profile lasting for 0.3 ms. Other than the laser irradiation, the entire structure was assumed to be insulated, allowing no convective or radiative cooling to the surrounding ambient environment. A typical FE mesh (containing around 60 000 nodes) is shown in Fig. 9.

Assuming no thermal contact resistance between the three-layer TIM specimen (using properties of the gap filler) and the sample holder plates, the temperature profiles of the rear coupon face inside the opening on the sample holder plate were averaged. The circular openings of both sample holder plates were 5.9 mm in radius. The temperature profiles are shown in Fig. 10 with distinct curves for aluminum, Lexan, and no holder plates.

By examining these curves it is possible to conclude that absorption of heat by the aluminum and Lexan sample holder plates led to a slower initial temperature rise than would have been experienced by the sample in the absence of these plates. While initially the rate of temperature increase was highest in the no-plate case, as shown in Fig. 10, the temperature reached the maximum value (within 90%) after 4–5 s due to the time for heat to flow through the three-layer sample. The half-rise time for the "no-plates" case was between 0.01 and 1.3 s, the range predicted by Parker's equation based on treating the three-layer composite structure composed of all TIM or all coupon material. The heat flux at a location along the opening edge of the top plate is shown in Fig. 11.

Heat flowed initially into the aluminum holder plates from the test sample due to the high plate thermal diffusivity. After

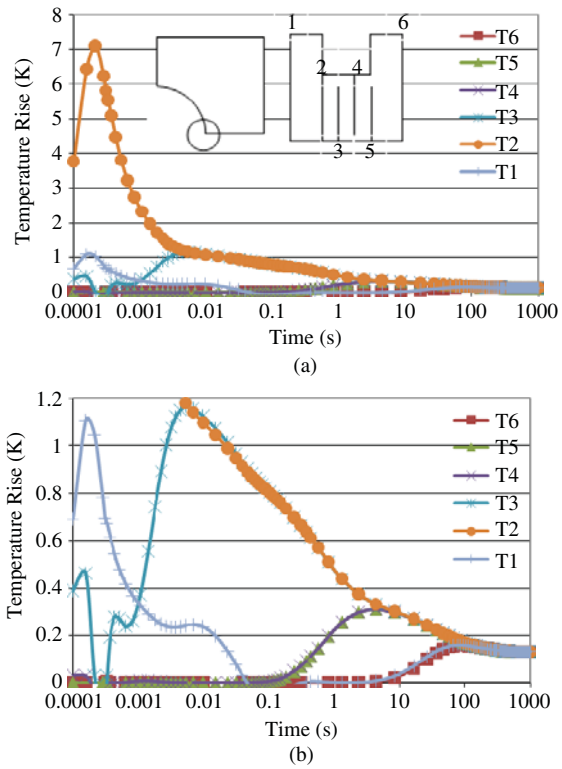

Fig. 12. Local temperature rise profiles throughout assembled test structure from laser flash simulations. (a) *y*-axis scale from 0 to 8 K. (b) *y*-axis scale from 0 to 1.2 K.

the aluminum plates became heated, thermal equilibrium was achieved when the heat flux from the three-layer sample in the plates reached a maximum and then decreased over time, causing the sample temperature to continue to rise gradually. For Lexan, heat flowed into the plates initially but at a slower rate than for aluminum. After the sample temperature reached a maximum point, the plates continued to draw heat away slowly because of the low thermal diffusivity of Lexan until the three-layer sample and plates reached a thermal equilibrium condition.

Fig. 12 shows nodal temperature profiles at multiple locations through the thickness of the assembly test structure (three-layer gap filler sample with Lexan plates). The nodal temperatures shown are located at the side of the assembly, as illustrated in the schematic in Fig. 12 (top view). In the side view, "T1" is closest to the side with the applied heat flux, and "T7" is on the opposite side of the test structure on the rear plate. The irradiated side of the coupon experienced the highest temperature rise, which peaked around the time of the applied heat flux. The bottom Lexan plate in contact with the irradiated coupon heated up initially and then decreased before being heated up by the test sample, while the top Lexan plate heated up more slowly after the temperature wave propagated through the three-layer test sample.

Since the entire simulated structure was insulated (except for the initial laser pulse), the final temperature was above the initial temperature. The temperature rise of the entire assembly at the steady-state condition (when the temperature no longer changed with time) depended on the specific heat capacity values, with the lower specific heat values corresponding to the higher steady-state temperatures. Using an energy balance and treating the three-layer sample and plates as a single system with no heat loss, the steady-state temperature rises from the simulation were calculated to be 0.32, 0.12 and 0.09 K, for no plates, Lexan, and aluminum, respectively, by summing the heat capacity contributions from all materials as well as lumped capacitance. These values were within 15% of the steady-state values from the FE simulation, which were 0.38, 0.13, and 0.09, respectively.

TABLE IV
CALCULATED TIM THERMAL CONDUCTIVITY BASED ON SIMULATION OF GAP FILLER ASSUMING NO CONTACT RESISTANCE BETWEEN THE TIM TEST SAMPLE AND SAMPLE HOLDER PLATES

Test specimen area (mm^2)	Plate material	Measured TIM thermal conductivity (W/m-K)	FEA TIM thermal conductivity (W/m-K)
147 (round)	Al	4.2	9.8
147 (round)	Lexan	3.2	2.9
147 (round)	None	N/A	2.7
320 (square)	Al	6.8	11.0
320 (square)	Lexan	3.6	3.2
320 (square)	None	N/A	2.8

Using the thermal properties of the gap filler, which had a datasheet thermal conductivity value of 2.8 W/m-K, simulations were performed with round and square test specimens. No thermal contact resistance was assumed between the TIM test sample and sample holder plates. Half-rise time values were based on the early part of the temperature rise profile, which resulted primarily from heating the test specimen rather than the sample holder plates. Due to the suppression of the sample temperature rise by the holding plates, the increase in TIM thermal conductivity was higher in the simulations with larger test specimens, which led to a larger area being in contact with the sample holder plates and higher in the simulations with aluminum plates compared to those with Lexan plates. The discrepancy between measured and simulated results in tests using the aluminum plate might have been largely due to the assumption of no contact resistance. Measurements with Lexan plates, however, showed a different trend: higher measured values than simulated values. This may have resulted from the actual TIM thermal conductivity being higher than the datasheet value used for the input value in the model. In addition, the Lexan plate samples may not have had the same plate-to-sample contact resistance as the aluminum plate samples during laser flash measurements. These results are summarized in Table IV.

Adding the same level of simulated plate-to-sample contact resistance (0.2 or 0.5 W/m-K contact layer with a 0.5 mm thickness) had a greater impact on TIM thermal conductivity values for the aluminum plate samples than for the Lexan plate samples, as shown in Table V. Since the aluminum plates were conductive, additional contact resistance significantly reduced the calculated TIM thermal conductivities due to sample holder plate heating (10.7–3.7 W/m-K by adding 0.5 W/m-K effective contact layers with 0.5 mm thickness). This did not greatly impact the Lexan plates, which were already relatively insulating.

TABLE V
CALCULATED TIM THERMAL CONDUCTIVITY BASED ON SIMULATION OF GAP FILLER A USING 320 mm^2 SQUARE SAMPLES WITH VARYING CONTACT RESISTANCE BETWEEN THE TIM TEST SAMPLE AND SAMPLE HOLDER PLATES

Contact layer thermal conductivity (W/m-K)	Plate material	FEA TIM thermal conductivity (W/m-K)
0.2	Al	3.2
0.5	Al	3.7
167	Al	10.7
0.2	Lexan	3.1
0.5	Lexan	3.2
2	Lexan	3.0

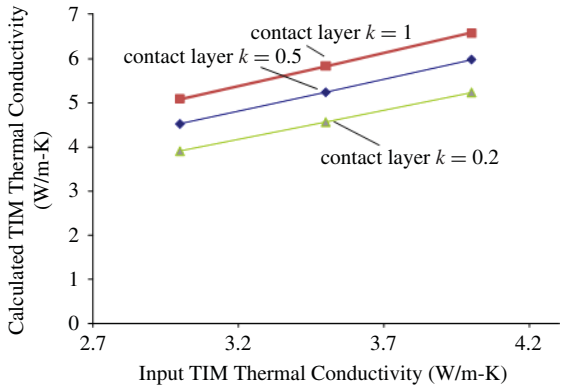

Fig. 13. Output TIM thermal conductivity based on FEA simulation with contact resistance as a function of input TIM thermal conductivity.

The mesh density of the thermal FE models was determined to be sufficient on the basis of a mesh sensitivity study carried out on gap filler (square sample) with a 1-mm bondline thickness and Lexan holder plates using two other meshes. The finest mesh (which contained 456 000 nodes) yielded a TIM thermal conductivity value of 3.3 W/m-K, which was within 3% of the value resulting from the model with a mesh density close to those used to obtain the other results.

Calculations of TIM thermal conductivity based on simulated temperature profiles thus indicated that sample holder plate heating increased TIM thermal conductivity values, matching the apparent trend found in laser flash measurements performed with aluminum sample holder plates. This result was produced because the laser flash method assumes that for thin test samples uniformly heated on one side, the half-rise time (time to reach one-half the maximum value) associated with the temperature rise on the opposite side is inversely related to the thermal diffusivity, as described by (2). Clamping the TIM specimens altered their temperature history considerably from the ideal laser flash test specimen conditions, which allowed heat flow through the three-layer specimen only. This resulted in lower slopes and more complex temperature-rise profiles. The equivalent half-rise times for clamped samples were highly dependent on the magnitude of the first local maximum temperature (first inflection point in the temperature profile).

The half-rise time was calculated using the first inflection point, since the laser flash instrument likely used the early part of the temperature-rise profile to calculate thermal diffusivity. This reference point was lower for the configurations experiencing a greater sample holder plate heating effect. For samples with aluminum plates, using the second inflection point in the temperature-rise profile would have resulted in TIM thermal conductivity values that were lower than those based on the first inflection point: 1.2 W/m-K rather than 11.0 W/m-K for the square samples, and 5.4 W/m-K rather than 9.8 W/m-K for the round samples. Since lower half-rise times resulted in higher thermal diffusivities, the TIM thermal conductivity values based on three-layer thermal diffusivity values were higher for configurations with a greater sample holder plate heating effect. This result has important consequences for reliability evaluation, since measured changes over time are experimentally determined as measured differences in TIM thermal conductivity at various instances in time, which would also be higher than actual changes in TIM thermal conductivity over time.

Even though sample holder plate heating should be avoided, using a plate design that reduces these effects may be difficult in some circumstances, for instance, when environmental conditions in a given reliability test and structural considerations also drive the plate material design and selection. Correcting for this effect requires performing a series of simulations to establish the relationship between input TIM thermal conductivity in the FE model, which corresponds to the actual value in a realistic case, and output TIM thermal conductivity from the FE model, which would be affected by sample holder plate heating. At least one accurate TIM thermal conductivity measurement obtained from a datasheet, an accurate alternative test method, or laser flash data obtained using a low-conductivity sample holder plate material could be used as the input TIM thermal conductivity in the FE model. The contact resistance between the test specimen and each plate can then be varied until agreement is achieved between the TIM thermal conductivity calculated from the FE model and the value used in the model (assumed to be accurate). Using this contact resistance value for a given TIM and loading condition, the input TIM thermal conductivity values can then be varied to obtain the relationship between the actual and the calculated TIM thermal conductivity values. This fitting approach assumes that the contact resistance between the test specimen and each plate does not change over time. For example, in measurements of Putty B using aluminum plates, the plots shown in Fig. 13 indicate that the slope of the curve determines how to correct for measured TIM thermal conductivity changes.

Generally, the lower the contact resistance between the three-layer laser flash test specimen and the sample holder plates, the lower the magnitude of the increase due to sample holder plate heating and the lower the slope (change in measured TIM thermal conductivity as a function of actual TIM thermal conductivity). Therefore, on Putty B samples, which showed a 1.8-W/m-K change after 2098 temperature cycles using aluminum sample holder plates, the actual change was up to approximately 1.2 W/m-K, i.e., a difference of 33% [31].

In the tests conducted and described in this paper and in the previous study [31], the screws holding the plates

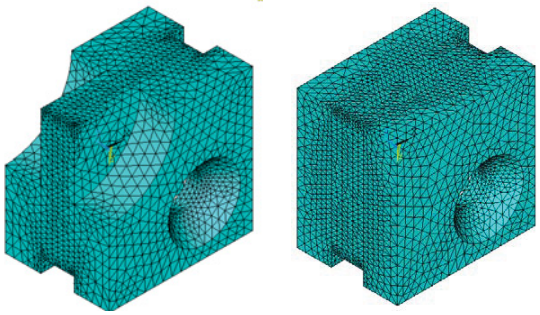

Fig. 14. Structural FE mesh (5.9 mm opening, 16.4 mm/side square test specimen) (a) open and (b) solid.

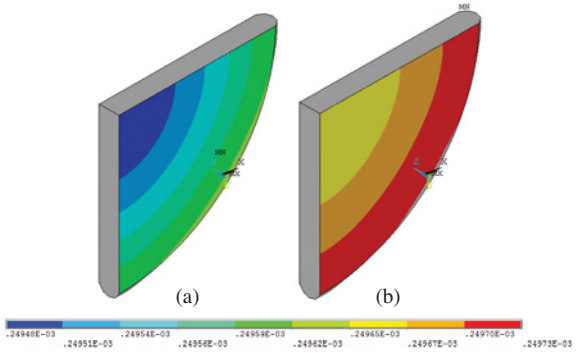

Fig. 15. z-Displacement (m) of Putty B at a 25% TIM compression level (a) open and (b) solid.

together restricted some movement of the plates, which were still free to move closer together over the course of the environmental exposure. Because of this aspect of the sample holder design, the contact resistance between the test sample and the clamping plates would have been likely to increase if the TIM layer experienced stress relaxation, which would have decreased the TIM bondline thickness over time. For any measured thermal performance degradation over time, the actual amount of degradation would have been lower than if the contact resistance remained constant since the measured value at the later time would have been closer to the actual value than the initial measurement.

As a result of stress relaxation in the TIM layer, the correction procedure described here would yield an upper limit in thermal performance change in cases of measured degradation. Sample holder plate heating effects would be present due to the possibility that later measurements would be conducted with increasing contact resistance between the sample and the plates. Overall, changes in the contact resistance between the test sample and the clamping plates over time limit the effectiveness of this correction procedure. This underscores the importance of avoiding sample holder plate heating by designing the sample holder plates accordingly.

The overall impact of sample holder plate heating can be reduced by using low contact pressure and a thermally insulating material for the sample holder plates with low thermal diffusivity and specific heat. TIM test coupons should only be slightly larger than the openings of the sample holder plates, minimizing the contact area between the holder plates and the test specimen such that the laser pulse area nearly covers the entire test specimen on one side during the laser flash measurement. If a high-conductivity material like metal is needed for the sample holder plates, a thin insulating layer could be added at the interface between the test coupons and the sample holder plates. Other sample holder plate shapes, such as a ring, may be possible as long as there is little contact between the plates and the test specimen.

B. Structural FE Simulations

Structural FE models have been used to simulate test samples as assembled for laser flash measurements, in which the three-layer samples were clamped using either Lexan or aluminum sample holder plates. Putty B and gap pad A were selected as representative TIMs to be modeled, and copper and alloy 42 were used as the coupons in the three-layer sandwich. To obtain the TIM shear modulus profiles, stress relaxation tests were performed using DMA in strain-controlled transient mode at room temperature. DMA test specimens were 4 mm $\times$ 4 mm in area, and the initial thicknesses of the Putty B and gap pad A specimens were 1 and 0.55 mm, respectively, matching the initial thicknesses in the simulated laser flash test structures.

The Prony series coefficients were generated in ANSYS based on the measured shear modulus profiles, and the resulting values were used to determine TIM material property inputs in the FEA model. In the FE models, screws were neglected, surface roughness was not considered between the TIM and the coupons, and clamping of the three-layer test specimens was simulated as a fixed constant displacement in the z-direction (through-plane) applied to the conical region at the top of one of the sample holder plates where the screw head would contact the sample holder plate. The bottom surface of the bottom sample holder plate (side opposite the applied force) was fixed. A free mesh was used with approximately 110 000 nodes and 80 000 elements. Solid187 (10-noded tetrahedral structural solid) elements were used in the model and two-axis sample symmetry (horizontal, vertical) was assumed. Sample meshes used for some Putty B simulations are shown in Fig. 14, where "solid" refers to geometries considered in a simulation that included plates with no openings.

Through-plane (z-direction) displacement in the top surface (the side with the applied force) of the TIM layer, which approximates the total deformation of the TIM due to compression, was used to quantify changes in the bondline thickness. Force was applied to the top surface of the top sample holder plate, and the bottom of the bottom plate was held fixed, causing the TIM layer to be compressed primarily from the top. The variation in the z-displacement was calculated as the difference between the maximum and minimum displacements at a steady-state condition (final time). For Putty B, which was clamped at a 25% compression level using Lexan plates with an opening radius of 5.9 mm, the z-displacement variation in the TIM was approximately 1.5×10^{-7} m, which was larger than the variation achieved with solid plates, i.e., 8×10^{-8} m,

TABLE VI
STEADY-STATE TIM z-DISPLACEMENT

TIM	% Compression (TIM layer)	Through-plane displacement variation of TIM Layer (m)	
		Open	Solid
Putty B	10	5.20E–08	3.00E–08
Putty B	25	1.50E–07	8.00E–08
Putty B	50	2.60E–07	1.50E–07
Putty B	75	4.70E–07	2.90E–07
Gap pad A	10	1.85E–06	1.20E-06
Gap pad A	25	4.20E–06	2.44E–06
Gap pad A	50	9.34E–06	6.10E–06

TABLE VII
STEADY-STATE TIM z-DISPLACEMENT OF GAP PAD A

Plate material	Radius of plate opening (mm)	Plate thickness (mm)	Through-plane displacement variation of TIM layer (m)	
			Open	Solid
Lexan	5.9	3.18	4.20E–06	2.44E–06
Lexan	2	3.18	2.98E–06	2.44E–06
Lexan	4	3.18	3.67E-06	2.44E–06
Lexan	8	3.18	3.30E–05	3.20E–05
Aluminum	5.9	3.18	2.41E–06	2.40E-07
Lexan	5.9	0.80	1.85E–06	1.20E–06

and was within 0.1% of the uncompressed bondline thickness. The z-displacement nodal contour plots of the TIM layer at the final time, shown in Fig. 15, indicate that the highest deflection was located near the outer edges of the test specimen, where the plates were in contact with the coupons.

Gap pad A simulations also showed the highest deflection near the outer edges of the test specimen. At the same compression level, the variation in the z-displacement of Gap Pad A (2.4×10^{-6} m for the solid case and 4.2×10^{-6} m for the open case, which was nearly 0.8% of the initial bondline thickness) was higher than for Putty B, but still small with respect to the initial thickness. The differences between the results with and without the openings were slightly larger, but they were still smaller than the experimental accuracy of a typical bondline thickness measurement (1×10^{-6} m). Simulations for both Putty B and Gap Pad A were carried out until 500 s, since the stress relaxation data showed that the elongation modulus of Putty B leveled off after that time. Simulations carried out until 1000 s indicated that 500 s was well within the steady-state range. The mesh density was determined to be sufficient based on a mesh sensitivity study carried out using two other meshes. The finest mesh (with 444 000 nodes and 310 000 elements) for the gap pad A simulation for the solid case at 25% compression level yielded a z-displacement variation of 3.7×10^{-6}m, which was within 11% of the result obtained using the other mesh.

Nodal contour plots of the z-displacement showed similar distributions in the TIM z-displacement at higher compression levels for both materials, and the displacement variation increased with increasing compression level. Assembly configurations for the open and solid cases matched each other well (within 1×10^{-6} m for Putty B, and 1×10^{-5} m for gap pad A) at multiple TIM compression levels from 10 to 75% when comparing variation in TIM z-displacement, as summarized in Table VI.

Varying the size of the openings in the sample holder plates caused the TIM layer to deform more uniformly in thickness with decreasing opening size for simulations of gap pad A at a 25% compression level. The z-displacement variation at a radius of 8.1 mm was around a factor of 10 higher compared to the results obtained using an opening radius of 5.9 mm. With aluminum holder plates at a 25% compression level, the variation in z-displacement with a 5.9-mm opening was around 60% lower than that with Lexan plates. Simulations with thinner Lexan plates, however, resulted in plate deflection, causing the overall compression level of the TIM layer to be much lower than the applied displacement. In experiments, this could lead to a test structure that deviates significantly from a typical loading condition and pose problems during assembling the test specimen. Results varying the plate opening size, material and thickness are summarized in Table VII.

Given these trends, a configuration with a large opening and coupon area, low stiffness plates, and a high-stiffness TIM layer would be expected to result in the most nonuniform deformation in the TIM. For a gap pad A sample compressed at 50% of the initial thickness and clamped using Lexan plates with an 8-mm radius opening, the variation in displacement of the TIM layer was found to be 3.3×10^{-5} m, which is still within 6% of the uncompressed bondline thickness. Even in this extreme case, the TIM remained relatively uniform in thickness, indicating that TIM specimens of similar dimensions, geometries, and moduli would also be suitable for laser flash measurements assembled in clamped three-layer structures. These results indicate that laser flash test structures can approximate typical TIM loading conditions that produce uniform bondline thicknesses.

VI. ANALYSIS OF UNCERTAINTY AND LEE METHOD NONCONVERGENCE

The overall experimental accuracy of the laser flash TIM thermal conductivity values, which depends on the error of each input in the Lee algorithm, can be affected by the design of the samples and the coupons that compose the three-layer test specimen. Since the thermal resistance values are derived, errors can propagate through both the laser flash measurement and the thermal resistance calculation. Lee [28] cautioned against using the laser flash method to measure the thermal diffusivity of a thin highly conductive material deposited on a low-conductivity substrate. For TIMs, this could be a concern when applying the laser flash method to a thin high-conductivity TIM, such as grease, gel, or solder, assembled in between thicker lower conductivity substrates or coupon layers.

In the Lee method [28] used in the TIM thermal conductivity calculation, the kth root of the characteristic equation

TABLE VIII
COMPARISON OF LASER FLASH MEASUREMENT ERROR

	Gap filler A	Putty B	Gel	Adhesive	Gap pad A
Experimental TIM thermal conductivity ± rms error (W/m-K)	6.5 ± 0.9	3.9 ± 0.4	6.7 ± 2.5	2.1 ± 0.7	2.1 ± 0.3
Experimental rms error (%)	14	10	37	34	16
Experimental $\eta_{1/2}$	0.2	0.1	1.5	0.3	0.2
Experimental $\eta_{3/2}$	1.0	0.5	8.2	1.7	0.9
Calculated maximum $\eta_{1/2}$	0.9	0.7	4.9	1.6	2.7
Calculated maximum $\eta_{3/2}$	4.7	3.5	26.4	8.3	14.6

(γ) must be determined in order to solve for the normalized temperature V, as follows:

$$\cot(\eta_1\gamma)\cot(\eta_2\gamma) + H_{1/3}\eta_{3/1}\cot(\eta_2)\cot(\eta_2\gamma) + H_{2/3}\eta_{3/2}\cot(\eta_3\gamma)\cot(\eta_1\gamma) - 1 = 0 \quad (5)$$

where η_i is the square root of the heat diffusion time through layer i, $\eta_{i/j}$ is the ratio of η_i to η_j, H is the volumetric specific heat, and $H_{i/j}$ is the ratio of H_i to H_j. The thermal diffusion time ratio can be defined as

$$\eta = \frac{l}{\alpha^{0.5}} \quad (6)$$

$$\eta_{1/2} = \frac{\eta_1}{\eta_2} \quad (7)$$

where 1 is the coupon 1 (copper), 2 the TIM layer, and 3 the coupon 2 (alloy 42). This is used to determine the normalized temperature V

$$V = 1 + 2\sum_{k=1}^{\infty} \frac{(\omega_1 X_1 + \omega_2 X_2 + \omega_3 X_3 \omega_1 X_4)\cdot Q(\gamma, \eta_3, t)}{\omega_1 X_1 \cos(\omega_1\gamma) + \omega_2 X_2 \cos(\omega_2\gamma) + \omega_3 X_3 \cos(\omega_3\gamma) + \omega_4 X_4 \cos(\omega_4\gamma)} \quad (8)$$

where the X_i terms are functions of H, the ω terms are functions of η_{ij}, and Q is a function of the heat pulse. The solution for γ, however, is highly sensitive to the thermal diffusion time ratios between the top or the bottom layer and the middle layer of a three-layer test specimen. Lee used thermal diffusion time ratios as criteria to determine when the layer was capacitive, in which the temperature was uniform throughout the layer. Some three-layer configurations can yield high root mean squared (RMS) errors in the calculated TIM thermal conductivity values obtained from the Lee algorithm or not result in a converged solution for the Lee algorithm. As a result, the selection of the material, bondline thickness, coupon material, and coupon thickness can affect the accuracy of calculated TIM thermal conductivity values and the ability of the Lee method to arrive at a converged solution. As an illustration, varying the three-layer thermal diffusivity and keeping all other inputs for the Lee algorithm constant effectively allows the TIM thermal conductivity to be varied. For a copper–gap pad A–alloy 42 composite test specimen, small changes in the η ratios lead to increasingly larger changes in the calculated TIM thermal conductivity values as the η ratios increase. Above around 190 W/m-K, the Lee algorithm does not result in a converged solution for a step size of 1×10^{-6}.

For measured samples in this paper, sensitivity of the calculated TIM thermal conductivity values to the η ratios led to varying levels of RMS error as calculated using the method described by Kline and McKlintock [34] and Moffat [35]. RMS error in calculated TIM thermal conductivity values reached 37% for the gel, which was the thinnest material with the highest conductivity in the group when assembled with 1-mm copper and alloy 42 coupons, as presented in Table VIII. By varying assumed hypothetical values of the three-layer thermal diffusivity and using all the same inputs used in the measurements, the calculated maximum $\eta_{\text{coupon/TIM}}$ values (the maximum values beyond which the Lee method produced nonconverged solutions for TIM thermal conductivity) was determined for each of the two coupon-TIM combinations per sample, as summarized in Table VIII. The maximum value for each η ratio pair varied from less than 4 to over 26, and values that led to converged solutions for one material did not result in converged solutions for others. While configurations with low η ratios may be more suitable for applying the Lee algorithm, the results suggest that acceptable η ratios may be material-dependent and that η ratios alone may not be sufficient for use as definitive criteria for determining the suitability of applying the Lee algorithm for all TIM types.

VII. CONCLUSION

Potential errors in interpreting laser flash measurements of TIM specimens assembled in three-layer sandwich structures and clamped using sample holder plates were examined. It was found that sample holder plates could achieve near-uniform loading over clamped three-layer sandwich structures, resulting in relatively uniform bondline thicknesses (usually within 1% variation in initial thickness for typical TIM compression levels) and can thus approximate as-assembled TIMs in many typical applications. However, heat from the laser pulse can flow into the holder plates during the laser flash measurement, which can increase the calculated TIM thermal conductivity

values obtained from thermal diffusivity data. To avoid this problem, low conductivity materials should be used for the sample holder plates, and the test specimens should be sized to match the opening of the sample holder plates. Since higher thermal diffusion time ratios between the TIM layer and the coupon layer appeared to lead to high overall error and problems with nonconvergence in TIM thermal conductivity calculations, thin conductive coupon layers should be used when laser flash measurements are performed on thin high-conductivity TIMs, such as gels or solder.

While the precautions that must be taken to avoid sample holder plate heating and error due to thermal diffusivity differences in the three-layer test sample may restrict how well an assembled laser flash test specimen simulates a realistic TIM application, the laser flash method can accommodate a wide range of TIM–coupon material combinations, surface roughnesses, and specimen sizes that match common die sizes in TIM applications. As a technique for reliability evaluation, the laser flash method may be an attractive alternative to steady-state ASTM D5470-based approaches [18] when used early on in the TIM selection process as a means of screening out TIMs based on their degradation behavior.

The thermal and mechanical considerations explored in this paper highlight the need for laser flash measurement standards, such as ASTM E1461 [30], to provide guidelines for measuring multilayer samples. Future work should focus on comparisons of laser flash data to data obtained using other techniques, including thermal test vehicles.

REFERENCES

[1] R. Prasher, "Thermal interface materials: Historical perspective, status, and future directions," *Proc. IEEE*, vol. 94, no. 8, pp. 1571–1586, Aug. 2006.

[2] C. Lasance, "The urgent need for widely accepted test methods for thermal interface materials," in *Proc. SEMITHERM XIX*, San Jose, CA, Mar. 2003, pp. 123–128.

[3] P. Rodgers, V. Eveloy, and M. G. Pecht, "Limits of air-cooling: Status and challenges," in *Proc. IEEE 21st Annu. Semicond. Thermal Meas. Manage. Symp.*, Mar. 2005, pp. 116–124.

[4] C.-P. Chiu, B. Chandran, K. Mello, and K. Kelley, "An accelerated reliability test method to predict thermal grease pump-out in flip-chip applications," in *Proc. 51st Electron. Compon. Technol. Conf.*, Orlando, FL, May–Jun. 2001, pp. 91–97.

[5] V. Gektin, "Thermal management of voids and delamination in TIMs," in *Proc. IPACK*, San Francisco, CA, Jul. 2005, pp. 641–645.

[6] W. Nakayama and A. E. Bergles, "Thermal interfacing techniques for electronic equipment-a perspective," *J. Electron. Packag.*, vol. 125, no. 2, pp. 192–199, Jun. 2003.

[7] M. M. Yovanovich, "Four decades of research on thermal contact, gap, and joint resistance in microelectronics," *IEEE Trans. Compon. Packag. Technol.*, vol. 28, no. 2, pp. 182–206, Jun. 2005.

[8] P. S. S. Abadi, C.-K. Leong, and D. D. L. Chung, "Factors that govern the performance of thermal interface materials," *J. Electron. Mater.*, vol. 38, no. 1, pp. 175–192, 2009.

[9] P. Rodgers, V. Eveloy, E. Rahim, and D. Morgan, "Thermal performance and reliability of thermal interface materials: A review," in *Proc. EuroSIME 7th Int. Conf. Thermal, Mech. Multiphys. Simul. Exper. Micrelectron. Microsyst.*, Milan, Italy, Apr. 2006, pp. 1–2.

[10] C. J. M. Lasance, C. T. Murray, D. L. Saums, and M. Rencz, "Challenges in thermal interface material testing," in *Proc. 22nd Annu. IEEE Semicond. Thermal Meas. Manage. Symp.*, Dallas, TX, Mar. 2006, pp. 42–49.

[11] A. Gowda, D. Esler, S. Paisner, S. Tonapi, and K. Nagarkar, "Reliability testing of silicone-based thermal greases [IC cooling applications]," in *Proc. 21st Annu. IEEE Semicond. Thermal Meas. Manage. Symp.*, San Jose, CA, Mar. 2005, pp. 64–71.

[12] R. Viswanath, V. Wakharkar, A. Watwe, and V. Lebonheur, "Thermal performance challenges from silicon to systems," *Intel Technol. J.*, vol. 4, no. 3, pp. 1–16, May 2002.

[13] I. M. Nnebe and C. Feger, "Drainage-induced dry-out of thermal greases," *IEEE Trans. Adv. Packag.*, vol. 31, no. 3, pp. 512–518, Aug. 2008.

[14] N. Goel, A. Bhattacharya, J. A. Cervantes, R. K. Mongia, S. V. Machiroutu, H. Lin, Y. Huang, K. Fan, B. Denq, C. Liu, C. Lin, C. Tien, and J. Pan, "Technical review of characterization methods for thermal interface materials (TIM)," in *Proc. Electron. Packag. Technol. Conf.*, vol. 10. Dec. 2008, pp. 1461–1471.

[15] E. C. Samson, S. V. Machiroutu, J. Y. Chang, I. Santos, J. Hermerding, A. Dani, R. Prasher, and D. W. Song, "Interface material selection and a thermal management technique in second-generation platforms built on Intel Centrino mobile technology," *Intel Technol. J.*, vol. 9, no. 1, pp. 79–80, Feb. 2005.

[16] B. Smith, T. Brunschwiler, and B. Michel, "Comparison of transient and static test methods for chip-to-sink thermal interface characterization," *Microelectron. J.*, vol. 40, no. 9, pp. 1379–1386, Sep. 2009.

[17] S. Somasundaram, A. A. O. Tay, and R. Kandasamy, "Evaluation of thermal resistance of TIMs in functional packages using a thermal transient method," in *Proc. Electron. Packag. Technol. Conf.*, vol. 10. Singapore, Dec. 2008, pp. 1479–1485.

[18] *Standard Test Method for Thermal Transmission Properties of Thin, Thermally Conductive Solid Electrical Insulation Materials*, ASTM D5470-01, Sep. 2001.

[19] J. P. Gwinn, M. Saini, and R. L. Webb, "Apparatus for accurate measurement of interface resistance of high performance thermal interface materials," in *Proc. 8th Intersoc. Conf. Thermal Thermomech. Phenom. Electron. Syst.*, May–Jun. 2002, pp. 644–650.

[20] J. R. Culham, P. Teerstra, I. Savija, and M. M. Yovanovich, "Design, assembly and commissioning of a test apparatus for characterizing thermal interface materials," in *Proc. 8th Intersoc. Thermal Thermomech. Phenom. Electron. Syst.*, San Diego, CA, May–Jun. 2002, pp. 128–134.

[21] C.-P. Chiu, J. G. Maveety, and Q. A. Tran, "Characterization of solder interfaces using laser flash metrology," *Microelectron. Rel.*, vol. 42, no. 1, pp. 93–100, Jan. 2002.

[22] R. C. Campbell, S. E. Smith, and R. L. Dietz, "Measurements of adhesive bondline effective thermal conductivity and thermal resistance using the laser flash method," in *Proc. 15th Annu. IEEE Semicond. Thermal Meas. Manage. Symp.*, San Diego, CA, Mar. 1999, pp. 83–97.

[23] W. J. Parker, R. J. Jenkins, C. P. Butler, and G. L. Abbott, "Flash method of determining thermal diffusivity, heat capacity, and thermal conductivity," *J. Appl. Phys.*, vol. 32, no. 9, pp. 1679–1684, Sep. 1961.

[24] R. D. Cowan, "Pulse method of measuring thermal diffusivity at high temperatures," *J. Appl. Phys.*, vol. 34, no. 4, pp. 926–927, Apr. 1963.

[25] L. M. Clark and R. E. Taylor, "Radiation loss in the flash method for thermal diffusivity," *J. Appl. Phys.*, vol. 46, no. 2, pp. 714–719, Feb. 1975.

[26] J. A. Koski, "Improved data-reduction methods for laser-pulse-diffusivity determination with the use of minicomputers," in *Proc. Int. Joint Conf. Thermophys. Proper.*, Gaithersburg, MD, Jun. 1981, pp. 94–103.

[27] H. J. Lee, "Thermal diffusivity in layered and dispersed composites," Ph.D. thesis, Dept. Mech. Eng., Purdue Univ., West Lafayette, IN, 1975.

[28] T. R. Lee, "Thermal diffusivity of dispersed and layered composites," Ph.D. thesis, Dept. Mech. Eng., Purdue Univ., West Lafayette, IN, 1977.

[29] J. Graebner, "Measuring thermal conductivity and diffusivity," in *Thermal Measurements in Electronics Cooling*, K. Azar, Ed. Boca Raton, FL: CRC Press, 1997.

[30] *Standard Test Method for Thermal Diffusivity of Solids by the Flash Method*, ASTM E1461-01, 2001.

[31] V. Khuu, M. Osterman, A. Bar-Cohen, and M. Pecht, "Effects of temperature cycling and elevated temperature/humidity on the thermal performance of thermal interface materials," *IEEE Trans. Dev. Mater. Rel.*, vol. 9, no. 3, pp. 379–391, Sep. 2009.

[32] J. D. Ferry, *Viscoelastic Properties of Polymers*, 3rd ed. New York: Wiley, 1980.

[33] P. Kohnke, "Viscoelasticity," in *ANSYS Theory Reference*. Canonsburg, PA: SAS IP, ch. 4.7.2, 2009.

[34] S. J. Kline and F. A. McClintock, "Describing uncertainties in single-sample experiments," *Mech. Eng.*, vol. 75, pp. 3–8, Jan. 1953.

[35] R. J. Moffat, "Describing the uncertainties in experimental results," *Exper. Thermal Fluid Sci.*, vol. 1, no. 1, pp. 3–17, Jan. 1988.

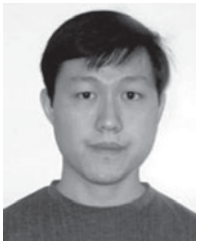

Vinh Khuu (M'06) received the B.S. degree from Stanford University, Stanford, CA, the M.S. degree from the Georgia Institute of Technology, Atlanta, and the Ph.D. degree from the University of Maryland, College Park, all in mechanical engineering.

He worked at the Northrop Grumman Corporation, Linthicum, MD, prior to his doctoral studies and is currently working at Schlumberger, Sugar Land, TX.

Dr. Khuu is a member of the International Microelectronics and Packaging Society and the American Society of Mechanical Engineers.

Michael Osterman (M'91) received the Ph.D. degree in mechanical engineering from the University of Maryland, College Park.

He is a Senior Research Scientist and the Director of the Electronic Products and System Consortium, Center for Advanced Life Cycle Engineering (CALCE), University of Maryland. He is involved in the development of simulation-assisted reliability assessment software for CALCE and simulation approaches for estimating time-to-failure of electronic hardware under test and field conditions. He is one of the principal researchers in the CALCE effort to develop simulation models for failure of Pb-free solders. He has been involved in the study of tin whiskers since 2002, and has authored several articles related to the tin whisker phenomenon. He has written eight book chapters and numerous articles in the area of packaging.

Dr. Osterman is a member of the American Society of Mechanical Engineers and the Surface Mount Technology Association. He received the Best Session Paper Award at the International Microelectronics and Packaging Society 41st Symposium in 2008, and the Best Paper-Maurice Simpson Technical Editors Award from the Institute of Environmental Sciences in 2008.

Avram Bar-Cohen (M'85–SM'87–F'93) is a Distinguished University Professor and Chair of mechanical engineering at the University of Maryland, College Park. He is the co-author (with A. D. Kraus) of *Design and Analysis of Heat Sinks* (New York: Wiley, 1995) and *Thermal Analysis and Control of Electronic Equipment* (Washington, NY: McGraw-Hill, 1983), and has co-edited nine books in this field. He has authored or co-authored some 300 journal papers, refereed proceedings papers, and chapters in books, and has delivered more than 60 keynote, plenary, and invited lectures at major technical conferences and institutions. He has been advisor to more than 50 Ph.D. and M.S. students at the University of Maryland, University of Minnesota, Minneapolis, and Ben Gurion University, Beersheba, Israel.

He is an Honorary Member of the American Society of Mechanical Engineers.

Michael Pecht (F'92) received the M.S. degree in electrical engineering and the M.S. and Ph.D. degrees in engineering mechanics from the University of Wisconsin, Madison.

He is the Founder and Director of Center for Advanced Life Cycle Engineering (CALCE), University of Maryland, College Park, which is funded by over 150 of the world's leading electronics companies at more than $6 million/year. He is also a Chair Professor in mechanical engineering and a Professor in applied mathematics at the University of Maryland. He has written more than 20 books on product reliability and development of chain management, and has published over 400 technical articles. He consults for 22 major international electronics companies, providing expertise in strategic planning, design, test, prognostics, internet protocol, and risk assessment of products and systems.

Prof. Pecht is a professional engineer. He is a world-renowned reliability engineer and educator. He was awarded the highest reliability honor, the IEEE Reliability Society's Lifetime Achievement Award in 2008. He received the IEEE Exceptional Technical Achievement Award for his reliability contributions in the area of prognostics and systems health management in 2010. He is a Fellow of the American Society of Mechanical Engineers, the Society of Automotive Engineers, and the International Microelectronics and Packaging Society (IMAPS). He has been a recipient of the European Micro and Nano-Reliability Award for outstanding contributions to reliability research, the 3M Research Award for electronics packaging, and the IMAPS William D. Ashman Memorial Achievement Award for his contributions in electronics reliability analysis. He served as Chief Editor of the IEEE TRANSACTIONS ON RELIABILITY for 8 years and on the Advisory Board of the IEEE Spectrum. He is Chief Editor for Microelectronics Reliability and an Associate Editor for IEEE TRANSACTIONS ON COMPONENTS AND PACKAGING TECHNOLOGY. The CALCE Center under him received the National Science Foundation Innovation Award in 2009.